ABSTRACT

Title of thesis: PRESSURE MEASUREMENTS FOR REFRIGERANT FLAMMABILITY LIMIT TESTING USING ASTM E681 APPARATUS

Alexandra Eve Klieger, Master of Science, 2017

Thesis directed by: Associate Professor Peter B. Sunderland
Department of Fire Protection Engineering

Improvements to the ASHRAE 34 and ASTM E681 standard test apparatus and procedure have been identified to make the test more repeatable and reproducible. Currently, the test apparatus centers around a glass flask with visual flammability criteria that can be subjective and dependent on a wide variety of factors. Additionally, the current test apparatus vents close to the time where the visual criteria is evaluated which can impact flame propagation.

A high frequency pressure transducer was added to the testing apparatus to understand the pressure development in the test vessel throughout flame propagation. Initial test pressures below atmospheric were studied to reduce the likelihood of premature venting. Quenching effects from the electrode rods of the test apparatus were quantified as well. Ultimately, a fractional pressure rise of 40% from a mixture starting at 91.2 kPa was proposed as a new pressure-based flammability criteria to potentially replace the current visual criteria. This new criteria would result in an lower flammability limit of 14.0% for R32.

PRESSURE MEASUREMENTS FOR REFRIGERANT FLAMMABILITY LIMIT TESTING USING ASTM E681 APPARATUS

by

Alexandra Eve Klieger

Thesis submitted to the Faculty of the Graduate School of the
University of Maryland, College Park in partial fulfillment
of the requirements for the degree of
Master of Science
2017

Advisory Committee:
Associate Professor Peter B. Sunderland, Chair
Assistant Professor Michael J. Gollner
Professor Emeritus James G. Quintiere

Acknowledgments

First and foremost, I would like to thank ASHRAE for sponsoring this project and giving us the freedom to explore many different aspects of the standard. Thanks to Dr. Peter Sunderland for his constant support and encouragement throughout this project and throughout my transition to Maryland.

This project would not be possible without our current research team: Jonathan Reymann and Dennis Kim. It has been immensely helpful to collaborate with both of them. Thanks to Markus Kokot for being a great intern and running tests with me for hours on end. I would also like to thank the previous research team that started this project and build a strong foundation for us: Vivien Le Coustre, Niko Thomas, Gauthier Pipard, Angela Hermann, Peter Lomax, and Conor McCoy. Extra thanks to Conor for answering my almost daily questions.

Thanks to the rest of the graduate students in the Fire Protection Engineering Department who have helped me with everything from LabVIEW to LaTeX and entertained me on countless study breaks.

Special thanks to Professors Michael Gollner and James Quintiere for serving on the advisory committee.

Finally, I would like to thank my family for supporting me through graduate school and giving me the confidence to take on new challenges.

Table of Contents

List of Tables

List of Figures

Chapter 1:   Introduction

1.1   Background

After the Montreal Protocol in 1987 and the United States Clean Air Act in 1995, there was a movement away from ozone depleting refrigerants, namely chlorofluorocarbon (CFC) compounds. By substituting the chlorine atoms with hydrogen atoms, the CFC refrigerant becomes a hydrofluorocarbon (HFC) with a reduced ozone depleting potential [1]. Further changes can reduce the global warming potential (GWP) but one side effect of this substitution is that the gas becomes flammable. Before fully adopting these new refrigerants, their flammability properties need to be characterized so that process safety and risk hazards can be evaluated. This new group is considered 'mildly flammable'.

Although a refrigerant/air mixture may be flammable, its behavior depends on many factors. If the gas is not able to sustain combustion, the mixture poses a negligible fire hazard. Knowledge of flammability limits is critical to the evaluation of risk and safety practices. Considerations need to be made for industrial process safety, manufacturing, transportation, and especially end use.

1.2 Purpose

This research is part of an ongoing research project conducted at the University of Maryland at College Park and sponsored by the American Society of Heating, Refrigeration, and Air-Conditioning Engineers (ASHRAE). The goal of this research is to improve repeatability and reproducibility of the ASHRAE 34 *Designation and Safety Classification of Refrigerants* testing standard for refrigerant flammability limits. This specific thesis centers around pressure measurements in the vessel throughout flame propagation to characterize venting, quenching effects, and flammability. The primary focus of this study is HFC refrigerants, emphasizing difluoromethane, CH_2F_2 (R32). R32 is representative of the newest class of refrigerants, 2L, as defined by ASHRAE 34.

The ASHRAE 34 test method utilizes the equipment and procedure from ASTM E681 *Standard Test Method for Concentration Limits of Flammability of Chemicals (Vapors and Gases)*. Two versions of the ASHRAE 34 [2] and ASTM E681 [3] experimental apparatus were constructed: one that meets the current guidelines of the standard and one with alternate construction materials. New instrumentation has been added to both to understand and quantify the behaviors of flame propagation, venting, quenching, and flammability as functions of concentration and initial test pressure.

1.3 Literature Review

Before discussing the current study regarding refrigerant flammability, a review of key terms, flammability standards, previous research, and current limitations must be done.

1.3.1 Common Definitions

ASHRAE: American Society of Heating, Refrigerating, and Air-Conditioning Engineers.

ASTM: Originally the American Society for Testing Materials, now operates as ASTM International.

Flame Propagation: the upward and outward movement of the flame front from the ignition source to the vessel walls (within 13 mm), as determined by visual observation [3].

Flammable Concentration Limit (FCL): the maximum allowable concentration of a gas in an industrial process setting, defined by ASHRAE 34 as 25% of the LFL [2].

Lower Flammability Limit (LFL): ASHRAE 34 defines this term as the minimum concentration of a refrigerant that is capable of propagating a flame through a homogenous mixture of the substance and air under specified test conditions [2].

Upper Flammability Limit (UFL): ASHRAE 34 defines this term as the maximum concentration of a refrigerant that is capable of propagating a flame through a homogenous mixture of the substance and air under specified test conditions [2].

1.3.2 Flammability Standards and Test Methods

Several different standards govern flammability limit testing. Schroder [4] identified the main factors to flammability as mixture composition, fuel, oxidizer, initial temperature and pressure, flow state, determination procedure, vessel type and size, ignition source, and direction of propagation. Standard testing methods can be divided into two main categories based on their determination of flammability: visual criteria and pressure criteria.

ASHRAE 34 [2] is the primary governing standard for the safety classification of refrigerants. It refers to ASTM E681 [3] for the flammability limit testing procedure. Additionally, it specifies test conditions of 23°C and 101.3 kPa. The experimental apparatus is a 12 L glass flask set inside an insulated chamber to control temperature conditions. ASTM E681 adopts a visual criteria measuring 90° between the igniter spark and the edges of the flame when the flame hits the vessel wall. The mixture is considered flammable if two out of three tests produce a flame wider than 90±5°. The standard states that the apparatus can be used for starting pressures as low as 13 kPa absolute.

Another ASTM International standard, ASTM E918-83 [5], outlines a standard practice for testing flammability limits of chemicals at elevated temperature and pressure, up to 200°C and 1.38 MPa. A metal vessel of at least 1 L is utilized for testing with a rupture disk for venting purposes. The standard defines a flammable mixture as one that yields a rise 7% above its original absolute pressure.

EN 1839 (T) [4], a European standard, evaluates flammability in an 80 mm

diameter glass cylinder. Flammability is determined by the visual detachment of the flame from the ignition source and a propagation greater than 100 mm. Another form of the standard, EN 1839 (B) [4] uses a closed 5 L bomb vessel with a 5% pressure rise criteria for flammability. Both of these standards label the last point of non-ignition as the LFL.

DIN 51649 [4] is a German flammability test standard that uses a 60 mm diameter glass tube, where the flammability criteria is a visual detachment of the flame from a high voltage spark ignition source. The LFL is the last non-explosion point after 5 repeated tests. Generally, European testing standards result in more conservative flammability limits.

In 2011, the United Nations called for a Globally Harmonized System (GHS) for the flammability of gases [6]. Their classification distinguished flammable gases into two categories. Category 1 gases are ignitable in a mixture of less than 13% by volume in air at atmospheric conditions or have a flammability range wider than 12%. Category 2 gases are all remaining gases that are flammable at atmospheric conditions. For this classification system, a clear definition of LFL and UFL are essential.

NFPA 69 [7] outlines the safety procedures for flammable gases in industrial process settings. The standard limits the allowable gas concentration of 25% of the LFL. This standard applies a safety factor on top of the LFL, but requires an accurate LFL determination.

1.3.3 Deficiencies in ASHRAE 34 and ASTM E681

Potential improvements to ASHRAE 34 and ASTM E681 are the focus of this current research. The primary deficiency in the ASTM E681 standard is the subjectivity of the visual criteria for flame propagation. The standard describes a mixture as flammable if the angle formed between the outer edges of the flame and the location of the igniter spark is at least $90\pm5°$ at the moment the flame hits the wall [3]. This criteria requires subjective assessment from the operator. No camera specifications, including sensitivity or recording frame rate, are specified in the standard. Flames for Class 2L refrigerants are weak and often faint as they propagate, leading to difficult assessments of the exact moment the flame hits the wall. Furthermore, as the glass flask begins to etch due to hydrofluoric acid (HF), a byproduct of Class 2L refrigerant combustion, the image becomes even more difficult to discern.

Lomax and McCoy [8, 9] conducted interviews with experts who frequently run this standard test. Technicians respected the simplicity and cost of the test, but expressed concerns that the 90° criteria is highly dependent on camera settings, positioning, and operator judgement. The ability to maintain a seal on the apparatus for tests conducted close to atmospheric pressure was also identified as a difficulty.

For materials with large quenching distances, like the refrigerants in question, ASTM E681 found a repeatability within a single laboratory within 0.2% for the LFL and 0.8% for the UFL. Between labs, however, reproducibility was within 0.9% for the LFL and 1.8% for the UFL [3].

1.3.4 Pressure Criteria for Flammability Limits

Standard test methods for flammability limits use both visual and pressure criteria. Pressure criteria is the primary focus of this work because of its simplicity and objectivity. Outside of the testing standards and refrigerant classification, a large body of literature exists regarding the use of pressure criteria for flammability limits of hydrogen, methane, and other hydrocarbons [4,10–14]. Pressure criteria are well established for hydrocarbon flammability.

Van der Schoor et al. [10] conducted tests of methane-air and hydrogen-air mixtures in a cylindrical vessel with a 5% pressure rise criteria for flammability. A direct relationship was found with a visual criteria with flame detachment and propagation of 100 mm. This comparison is the foundation for the EN 1839 (T) and (B) standard.

Zlochower et al. [11] examined the flammability of methane, propane, ethylene, carbon monoxide, and hydrogen in a 12 L ASTM E681 vessel with visual criteria in a 120 L closed spherical vessel. Explosion pressure increased slowly with concentration until an overpressure of 7% was observed, after which explosion pressure increased significantly with increasing concentration. There was good agreement between the visual method in the 12 L vessel and pressure definitions of flammability from the 120 L closed vessel.

Crowl and Jo [12] used a less traditional pressure description of flammability by examining the second derivative of pressure. This description was less arbitrary than a simple pressure rise because it described the acceleration of heat release rate

and was more fundamentally based. The results were more conservative than other methods. However, signal to noise ratio suffers with each derivative.

Liu and Zhang [13] studied the influence of starting temperature and pressure on the flammability limits of hydrogen in a 5 L closed steel cylinder. A 7% pressure criteria was adopted. They found that the flammability range widens with both increasing temperature and starting pressure. All tests were conducted at or above atmospheric pressure. Similarly, Li et al. [14] found that flammability range decreased with decreasing temperatures through testing of methane. Li used a 100 mm diameter stainless steel cylinder with temperatures at and below ambient room temperature.

Schroder and Molnarne [4] conducted testing to compare the flammability limits of hydrogen, ethylene, methane, and ammonia in air. Tests were performed according to DIN 51649, EN 1839 (T), EN 1839 (B), and ASTM E681. Up to 1.1% variation was found in LFL depending on the method and pressure measurements resulted in the least conservative limits for these gases.

1.3.5   Refrigerant Classifications

The focus of this research will be on Class A2L refrigerants, as defined by ASHRAE 34 [2]. All experiments were performed with R32 because it is representative of an A2L refrigerant.

Class A: toxicity classification for a refrigerant with an Occupant Exposure Limit of 400 ppm or greater.

Class 1: flammability classification for a refrigerant demonstrating no flame propagation when tested at 60°C and 101.3 kPa.

Class 2: flammability classification for a refrigerant demonstrating flame propagation at 60°C and 101.3 kPa, an LFL greater than 0.10 kg/m^3, and a heat of combustion less than 19,000 kJ/kg. Some other standards present the LFL as a mole fraction instead.

Subclass 2L: a further classification for refrigerants with a maximum burning velocity of 10 cm/s at 23°C and 101.3 kPa.

Class 3: flammability classification for a refrigerant demonstrating flame propagation at 60°C and 101.3 kPa, an LFL less than or equal to 0.10 kg/m^3, and a heat of combustion greater than 19,000 kJ/kg. Some other standards present the LFL as a mole fraction instead.

1.3.6 Combustion of R32

The combustion of R32 is the centerpiece of this research and the basics of this combustion process were reviewed.

The stoichiometric mole fraction for the combustion of R32 in air is 0.1736. At stoichiometric composition, where all reactants are converted into products without any incomplete combustion, R32 (CH_2F_2) reacts as

$$CH_2F_2 + (O_2 + 3.76\,N_2) \longrightarrow CO_2 + 2\,HF + 3.76\,N_2. \tag{1.1}$$
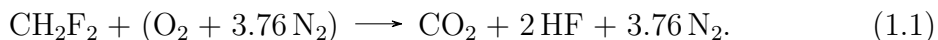
Hydrogen fluoride (HF) is a toxic chemical, especially when combined in solution

with water. The chemical is hazardous to human health and rapidly etches glass. As Equation 1.1 shows, the amount of water produced by dry combustion of R32 is negligible — two orders of magnitude lower than the other combustion products [15]. The stoichiometric laminar flame speed for R32 is 6.7 cm/s. R32 mass is 0.052 kg/mol, which is almost twice air. The boiling point is -51.7°C at 101 kPa [15].

1.3.7 Flammability Testing of R32

The LFL of R32 was examined thoroughly as a foundation for this research. A selection of values for the lower flammability limit of R32 are reported in Table 1.1:

Table 1.1: Reported LFL for R32

LFL	Ref.	Conditions	Apparatus
13.5	[16]	20°C, 0% RH, 0.4 s spark	ASTM E681
13.8	[17]	20°C, 0% RH, 0.4 s spark	5 L steel explosion vessel
14.0	[18]	Not specified	Dupont MSDS
14.0	[15]	35°C, 0% RH	Twin counterflow flame
14.4	[1]	23°C	ASTM E681
14.4	[19]	Ambient room conditions	20 L explosion sphere
14.7	[18]	Not specified	Allied Signal MSDS
14.7	[8]	21-23°C, 0% RH, 0.2 s spark	ASTM E681 with burst disk
14.8	[8]	21-23°C, 0% RH, 0.2 s spark	ASTM E681 with stopper
15.2	[20]	20-22°C, 0% RH, 10 mA spark	ASTM E681 extrapolated

Kul et al. [20] performed experiments on R32 in four different vessels to address the impact of vessel size on flammability limits. They determined that quenching effects are significant for mildly flammable refrigerants, but these effects are negligible once a minimum size of 5 L is used. After extrapolating flammability limits to a vessel of infinite size, they reported an LFL for R32 at 15.2%. This value was consistent with Richard's [21] results for a 200 L vessel.

Lisochkin and Poznyak [22] studied the effects of starting pressure on flammability limits in a stainless steel cylinder at 60°C. As starting pressure increased, the flammability range widened. The pressure rise and rate of pressure rise also increased with increasing starting pressure. At atmospheric pressure, they reported an LFL of 13.5±0.5% for R32 at 60°C.

Zhang et al. [19] examined the flammability limits of R32 with a 20 L explosion apparatus. They reported an LFL of 14.4% and documented a rate of pressure rise close to 35 MPa/s near the LFL.

Kondo et al. [16, 17] studied refrigerant flammability extensively. One study examined the impact of starting pressures on the flammability of R32, R1234yf, and methane. They utilized a 5 L stainless steel vessel with a 20% pressure rise criteria for flammability. This criteria was derived from the 90° fan criteria in ASTM E681. A 90° fan corresponds to approximately 30% of the volume of the sphere. The volume of burned gas is the primary factor towards pressure rise, so a 20% criteria is representative of this situation. LFL of R32 was reported as a function of starting

pressure in kPa:

$$L = 11.70 - 1.3 * \ln(\frac{p}{500}), \tag{1.2}$$

relating to 13.8% at 101 kPa [17]. Kondo also performed experiments in a 12 L ASHRAE sphere using visual criteria. An LFL was reported at 13.5% at 20°C with no effects from humidity.

An alternative experiment was created by Grosshandler and co-workers [15,23, 24] to derive flammability limits as a fundamental material property instead using an imposed cutoff criteria. They utilized a counterflow twin-flame burner and measured strain rate at extinction in the flames at various concentrations. A flame near its LFL will extinguish with less added strain rate than a stoichiometric flame. The strain rate was extrapolated to a zero-case as a function of concentration, representing the lower flammability limit as a physical property. They reported an LFL for R32 at 12±0.6%. They used the same method with a more refined apparatus and reported an LFL of 14% at 35°C and 13.1% at 100°C. Additionally, they found no effect of the flammability limit as a function of relative humidity.

One of the most comprehensive studies on R32 flammability was conducted by Heinonen and Tapscott [18,25] . They addressed discrepancies and ambiguities that resulted from comparisons between the ATSM E681 apparatus and an explosion sphere. The explosion sphere utilized a 7% pressure rise criteria. In their conclusion, they made recommendations for the ASTM standard. These recommendations included the incorporation of a microphone to indicate the time of venting, as well as the incorporation of a pressure gauge to compare visual criteria to pressure rise in

the 12 L flask. Additionally, they suggested testing flammability below atmospheric to allow for more reproducibility between laboratories at different elevations.

1.4   Introduction Summary

The ASHRAE 34 and ASTM E681 standard test apparatus and procedure must be modified to make the test more repeatable and reproducible. Currently, the test apparatus centers around a glass flask with visual flammability criteria. Visual criteria can be subjective and dependent on a wide variety of factors including frame rate, aperture settings, brightness, and critical frame selection. These factors can lead to variability between testing laboratories, different operators, and different testing series. Adding a pressure transducer may allow the visual method to be confirmed or replaced.

There is evidence based on existing standards that flammability criteria derived from pressure can reliably determine flammability limits for many gases, including refrigerants. Pressure measurements have not been well documented for the ASTM E681 apparatus specifically. Furthermore, no pressure-based criteria has been identified to appropriately replace the visual criteria without disrupting the widely accepted flammability limits determined to date by ASTM E681. The goal of this research is to fill these gaps and pave the way for future flammability test methods for mildly flammable gases.

Chapter 2:   Experimental Apparatus

2.1   ASTM E681 Apparatus and Modifications

The majority of experiments were conducted in a modified version of the ASTM E681 apparatus with a polycarbonate vessel, as illustrated in Figure 2.1. The main deviation from the standard apparatus was the flask material. The body of the glass flask was replaced with a polycarbonate sphere and the neck of the flask was replaced by a combination of polyvinylchloride (PVC) sheet and PVC tube. A weighted rubber stopper was used to control venting. For details, see Reymann's thesis [26].

Preliminary baseline experiments were performed in a 12 L glass apparatus, compliant with ASTM E681, with a modified burst disk venting system. Apparatus photos are included in Appendix A. The apparatus was originally designed by Lomax [9]; the burst disk to control venting was designed by McCoy [8]. Full details of the design and construction are elaborated in their respective theses.

Figure 2.1: Polycarbonate apparatus

The polycarbonate apparatus has several benefits over the glass design. The main benefit is that the polycarbonate does not etch at all, while the glass is irreparably etched after 5-10 tests. Additionally, the polycarbonate can be easily drilled and the electrodes were arranged as penetrations through the side of the vessel instead of coming through the neck of the flask. In his masters thesis, Reymann [26] proves the equivalency for polycarbonate and glass at room temperature and near-atmospheric pressures. Reymann also further discusses the construction and benefits of this system.

Both test configurations utilized the same ignition system to generate a 15 kV spark at 30 mA. The duration of the spark was 0.2 s, shortened from the common

0.4 s. The standard allows for either spark duration, but the duration of flame propagation was found to be approximately 0.4 s, so a spark of that length would overdrive flame propagation.

The two setups shared the same plumbing system. Instrumentation was added to both configurations to quantify venting as well as examine pressure measurements associated with flammability.
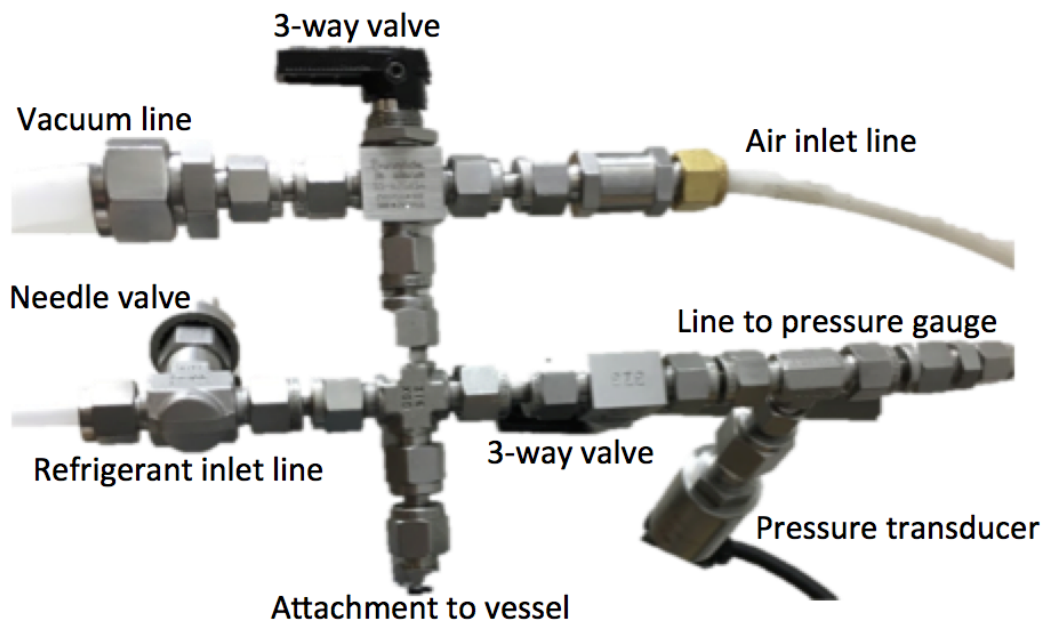

Figure 2.2: Labeled plumbing tee

The plumbing tee had four lines: one for the vacuum pump; one for the air inlet; one for the refrigerant inlet; and one for the low frequency pressure gauge and high frequency pressure transducer, as illustrated in Figure 2.2. Lomax described the full details of the original plumbing system construction [9].

2.2 Instrumentation

2.2.1 High Speed Camera

A Casio Exilim high speed camera (EX-FH100) was used to record each test. The camera was set to 120 fps and the other settings were held constant for each trial. The videos were used to analyze the visual propagation of the flame and to calculate the flame angles for the ASTM E681 flammability criteria. The camera was positioned outside the fume hood to protect the camera lens from HF and other combustion byproducts.

2.2.2 Low Frequency Pressure Gauge

A low frequency pressure gauge was utilized for filling the vessel with a known concentration of refrigerant. ASTM E681 requires the installation of a low-range pressure gauge such as this one [5]. As a note, ASTM E681 uses the terms 'gauge' and 'transducer' interchangeably, but in this report, 'gauge' will only refer to the low frequency pressure gauge; likewise, the term 'transducer' will only refer to the high frequency pressure transducer described in Section 2.2.3.3. A partial pressure method was adopted to fill the vessel after it had been thoroughly evacuated by the vacuum pump. Partial pressure was calculated using

$$\frac{p_i}{p_{tot}} = X_i, \tag{2.1}$$

where p_i was the pressure of one component; p_{tot} was the total pressure of the mixture; and X_i was the volume fraction of one component in the total. Absolute pressures must be used for this calculation.

First, a vacuum was pulled in the vessel. Then, refrigerant was introduced to the vessel. Afterwards, air was added until the desired starting pressure for the test was reached. The mixture was then stirred for five minutes to ensure homogeneity. Per the standard requirements, ignition was attempted within one minute of turning the stirrer off. This minimized the effects of turbulence without allowing for leakage.

The low frequency pressure gauge was mounted to the control panel, as shown in Figure 2.3.
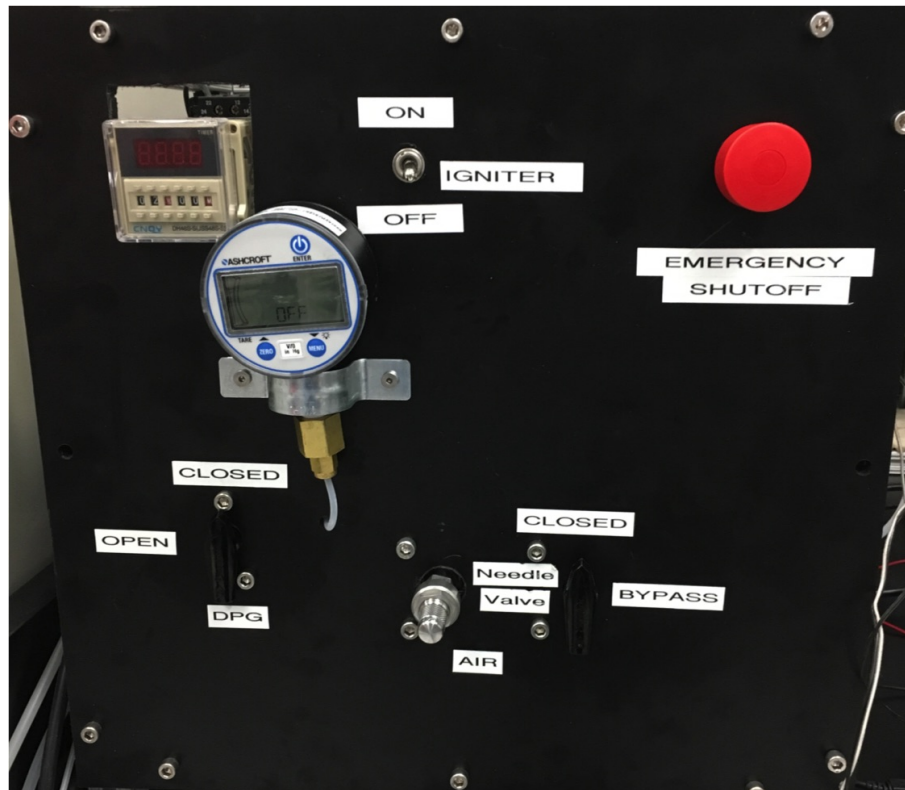
Figure 2.3: System control panel

The gauge was a Ashcroft digital vacuum gauge (DG25). The gauge was

calibrated for accuracy within a range of 0-101.6 kPa absolute pressure. Combining

the gauge uncertainty with the effects of long term leak rate and the steady state

settling time, the concentration of refrigerant was considered accurate within 0.1%.

2.2.3 Data Acquisition System

A data acquisition system (DAQ) from National Instruments (NI USB-6001) was

incorporated into the experimental system to record the voltage readings from a

switch, microphone, and a high frequency pressure transducer. The unit is shown

in Figure 2.4 with a wiring diagram in Figure 2.5.

Figure 2.4: National Instruments data acquisition box

Figure 2.5: Data acquisition wiring diagram

The data acquisition box had 8 analog input channels, 2 analog output channels, and 13 digital input and output channels. Moreover, it was capable of outputting a steady 5V DC signal and the box was powered through a USB connection to a laptop. The data acquisition system reco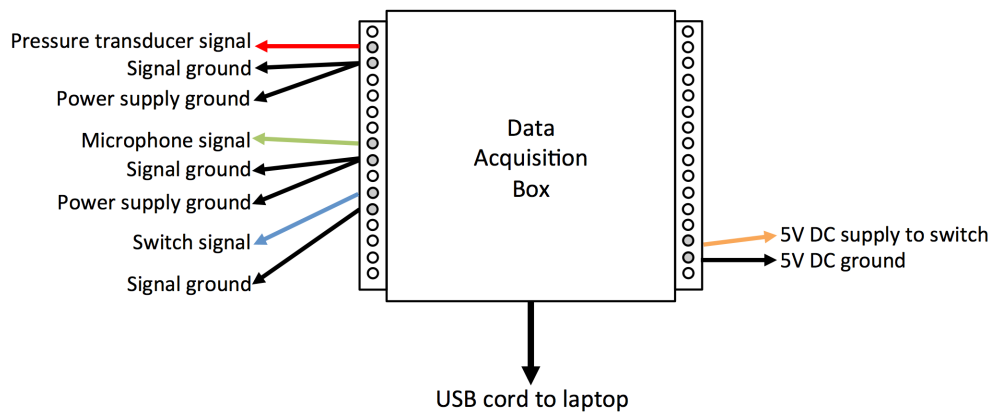rded all data channels at 500 Hz through LabVIEW software (2015 edition). The DAQ recorded all three inputs simultaneously, so signal synchronization was automatic.

2.2.3.1   Switch

A single switch was used to operate two circuits simultaneously. The switch was purchased from McMaster Carr (#7343K253) and installed on the control panel, as shown above in Figure 2.3. It controlled the circuit for the spark gap igniter and a second circuit for DAQ measurement of switch activity. The second circuit was wired from the 5V supply from the DAQ, through the switch, and back into an analog input for the DAQ. This second circuit allowed for a direct signal into the data recording system for the activation of the spark igniter. This moment was considered the initiation of flame propagation for analysis purposes and synchronization with the high speed video.

2.2.3.2   Microphone

An Adafruit Electret Microphone Amplifier (MAX4466) was wired into the data acquisition system to record the sounds of the spark and venting from the vessel. The microphone does not allow playback, but collects voltage measurements as a

function of time. The microphone output allowed for accurate time records for major sound events. The microphone was positioned near the apparatus on a separate stand, as demonstrated in Figure 2.6.

Figure 2.6: Two microphones positioned near the polycarbonate vessel

ASTM E681 cautions the operator to shield instrumentation from any electrically conductive paths that could be in close proximity to the spark generator [5]. The stand was carefully isolated from the apparatus because the radio frequency (RF) burst that occurred with the high voltage spark turned nearby metal into an antenna which could burnout the microphones amplifier if the microphone wires were not properly protected.

2.2.3.3   High Frequency Pressure Transducer

The key instrumentation to identify possible pressure criteria for flammability was a high frequency pressure transducer. A thin film pressure transducer was selected

for its combination of accuracy and response time. The selected model was from PCB Piezoelectronics in the 1500 series (#1501B02EZ100PSIG) and it was rated for 0-690 kPa gauge (0-100 psig), though it provided accurate measurements as low as -34 kPa gauge (-5 psig). The transducer could operate between -40 and 125°C with <1 ms response time. Typical flames in the apparatus lasted less than half a second, so this response time is crucial. Measurement resolution was accurate within ± 0.07 kPa.

The high frequency pressure transducer was mounted onto the plumbing tee, on the same line as the low frequency pressure gauge, as shown in Figure 2.2. A valve was installed before the transducer to close off the line during the full venting process, as seen in Figure 2.7. This protects the transducer from corrosive hydrofluoric acid that may damage the device after long term exposure.

Figure 2.7: Valve installed to protect the pressure transducer

Pressure measurements were recorded at 500 Hz and smoothed with a 10-point running average to reduce noise. A comparison of raw data and smoothed data can

be seen in Figure 2.8. The raw data is noisy and difficult to interpret. The 20-point running average smooths the data thoroughly, but the peak pressure values are lost. The 10-point running average eliminates the high levels of noise from the transducer, without losing the peak of the pressure curve.
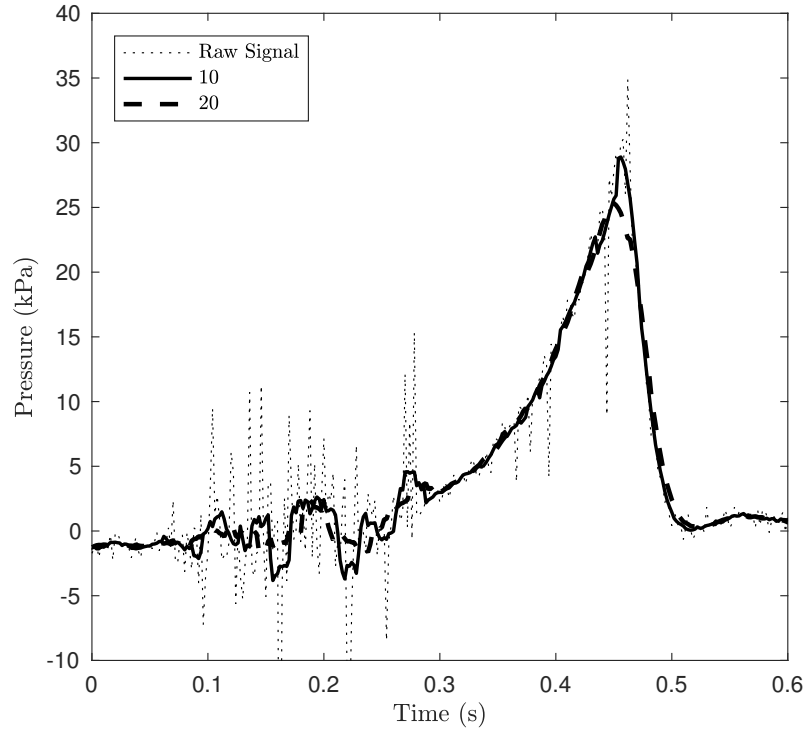
Figure 2.8: Smoothing effects

2.2.4 Additional Microphone

A simple 3.5 mm auxiliary jack lapel microphone (HDE #240173) was utilized for many of the tests to quantify the difference in time between when the flame hits the wall and when the vessel vents. The two different microphones were recorded side-by-side from a stand near the vessel, as shown in Figure 2.6.

This microphone was recorded with Garageband software. The benefit of this

microphone over the DAQ microphone was that it allowed audible playback instead of just a voltage measurement. The two microphones showed similar key events at the same times, but the DAQ microphone was more quantifiable for analysis than the simple lapel microphone. The lapel microphone was ultimately abandoned once sufficient confidence was built in the Adafruit microphone.

2.3   Experimental Conditions

All experiments were performed at room temperature (21-23°C) with 0% relative humidity inside the vessel. Measurements were taken for initial starting pressures of 81.1 kPa (0.8 atm), 91.2 kPa (0.9 atm), and 101.3 kPa (1.0 atm) to understand the impact of initial pressure on flame propagation and vessel venting behavior. All experiments were performed with R32 because R32 is a widely used refrigerant that is representative of the 2L classification.

Chapter 3: Results and Discussion

3.1 Venting Measurements

The first objective of the audio and pressure measurements was to quantify the moment of venting and understand the influence of venting on flame propagation. The majority of experiments were conducted in the polycarbonate apparatus and are discussed in this chapter, but an analysis of venting in the glass apparatus is included in Appendix A.

Venting was originally characterized through the sound signature of rushing air, but ultimately, pressure measurements were sufficient to identify when the propagating flame was affected by venting. The plots in Figure 3.1 are representative of a typical flame propagation. These specific plots are extracted from a test with 15% R32 at 91.2 kPa starting pressure. All three plots are lined up on the same time scale for comparison.
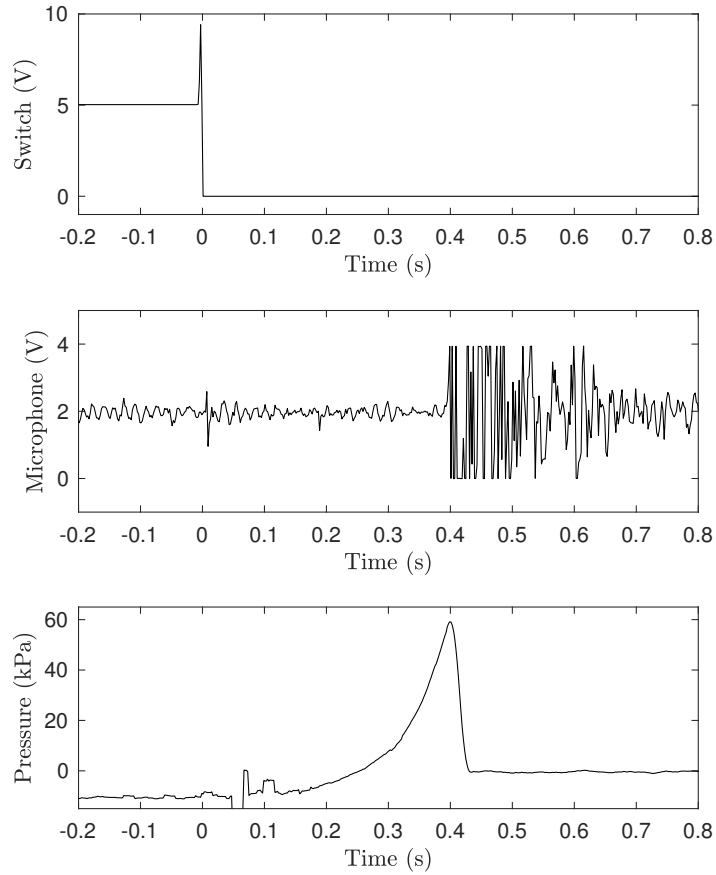
Figure 3.1: Measurements for 15% R32 at 91.2 kPa starting pressure: switch (top), microphone (middle), and pressure transducer (bottom)

Background audio conditions and initial pressure conditions are recorded before the spark occurs, indicated by time less than zero seconds. The first notable event happened at the 0 s mark. This was when the spark gap igniter is activated. This was illustrated most clearly in the top plot, which shows the activation of the igniter switch. At this time, a blip is seen on the middle microphone plot, representing the initial sound of the spark. Finally, on the bottom plot, this moment is seen as the start of the pressure rise. The spark is active for 0.2 s so it is possible that

the mixture is not ignited at the first instance of the spark, but it is not feasible to pinpoint the start of propagation any more specifically than the initiation of the igniter.

The second key event happened at about 0.4 s on the plot; this was the moment of venting. On the microphone plot, a surge in voltage is seen, representing the rush of sound heard upon the stopper ejecting from the vessel. After an initial loud pop, the sound level returned to a background level, though the background level was louder than the ambient sound before ignition. This was explained by the air flush being introduced to purge the vessel of HF and other combustion byproducts. The moment of venting on the microphone plot lined up perfectly with the moment of peak pressure. Pressure rose until the weighted stopper could no longer contain the pressure inside the vessel.

Because the audio and pressure traces lined up, either venting audio or peak pressure could have been used to indicate the moment of venting. The moment of peak pressure was used as the indicator of venting for data processing because it was more reliable and less affected by ambient conditions inside the fume hood.

Venting time was measured between the moment the igniter switch was activated to the moment maximum pressure was achieved. The instance the flame reaches the wall was evaluated visually and the time was calculated by counting the number of frames between the first sight of the spark and the flame reaching the wall. The time difference between the flame reaching the wall of the vessel and venting were typically within 0.2 s of each other. To better distinguish between these events, different starting pressures were examined. A series of measurements were taken for

starting pressures of 81.1, 91.2, and 101.3 kPa. Theoretically, with lower initial pressures, a longer duration of the flame would be captured inside the vessel prior to venting. With initial pressures near atmospheric, the flame propagation itself would not be significantly affected by pressure. Some pressure-based flammability tests occur in a fully closed steel vessel, but the ASTM E681 standard calls for an apparatus that vents at comparatively lower pressures to protect the integrity of the glass and to represent the constant-pressure conditions that would normally occur in a residential explosion. An examination of starting pressures sought to find a balance between capturing the full duration of the flame propagation and distorting the flame from atmospheric propagation.

The timing differences between the flame reaching the walls of the vessel and the vessel venting are shown in Figure 3.2 for absolute starting pressures of 81.1, 91.2, and 101.3 kPa. All experiments for this analysis were conducted in the polycarbonate apparatus so that the trials were all directly comparable and consistent. The flame reached the vessel wall between 0.3 and 0.4 s after ignition for almost every R32 flame, regardless of starting pressure.

A series of assumptions was made to use this data to calculate a first-order accurate laminar flame speed. Buoyancy was assumed to be the only thing driving the flame upward and laminar flame speed was assumed to be the only factor driving the flame outward. More complicated analysis of buoyancy, flame stretch, and curvature was not considered.
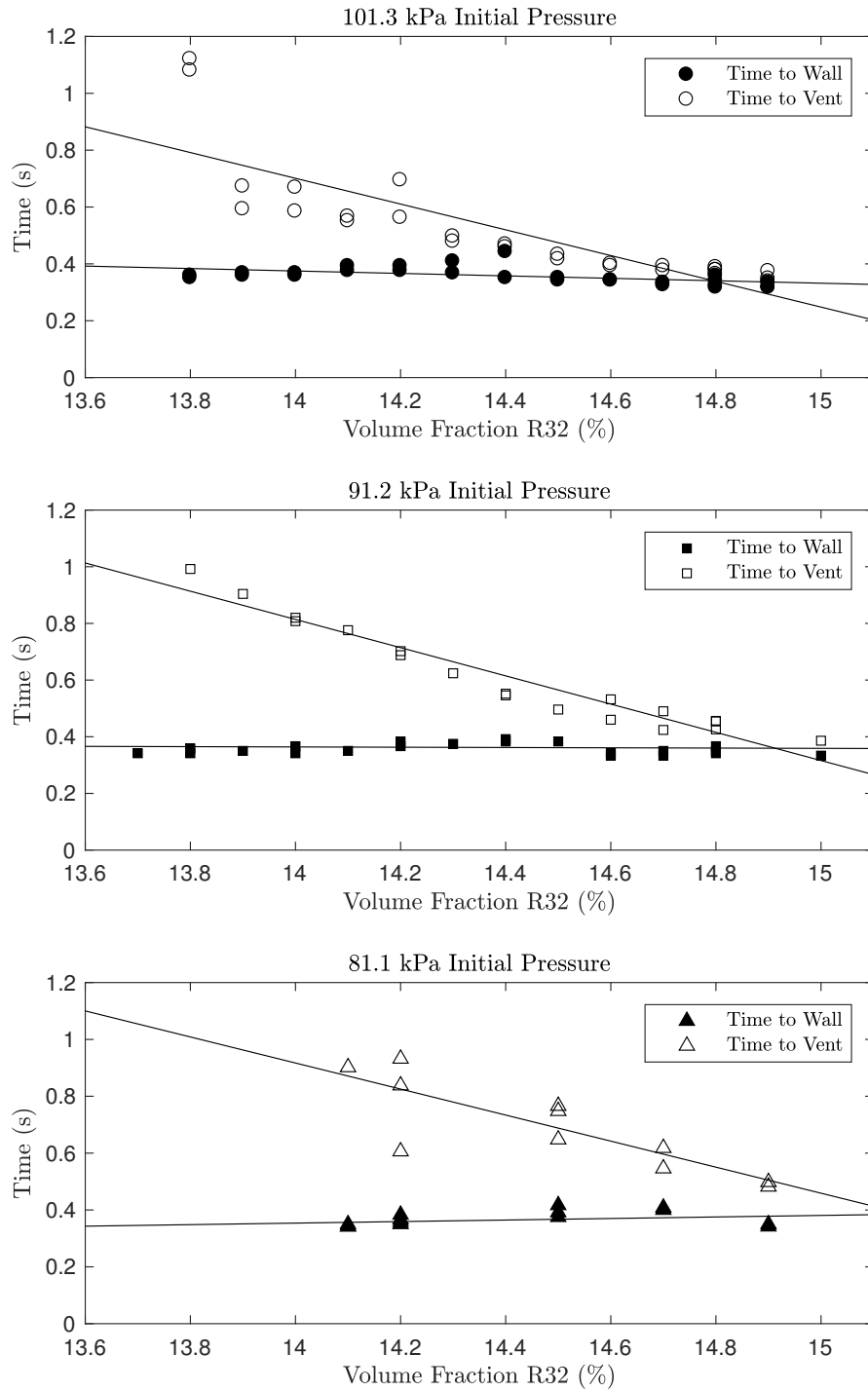
Figure 3.2: Measurements for the time when the flame reaches the wall and when the vessel vents
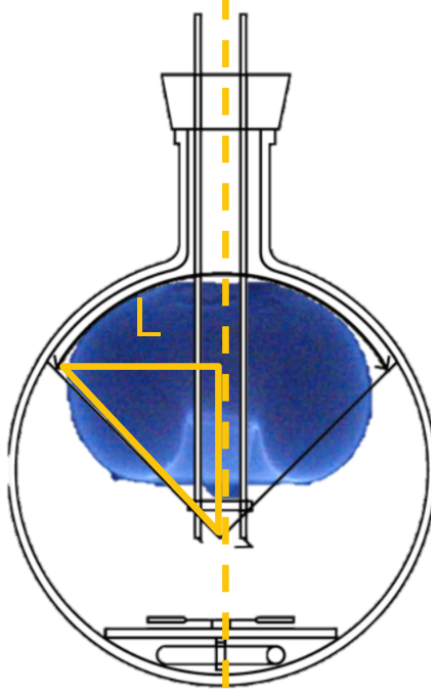
Figure 3.3: Simplified calculation of laminar flame speed

By taking the outward distance traveled, marked L in Figure 3.3, and dividing this by the time to reach the wall, an approximate laminar flame speed of 17.8 cm/s was calculated.

$$S_L \approx \frac{L}{t} = 17.8 \ cm/s \tag{3.1}$$

This was a factor of three higher than the laminar flame speed for R32 and the effects of concentration were considered negligible on such a small concentration range. More accuracy could be obtained by correcting for buoyancy and spherical propagation. This suggests that the starting pressure does not have a significant effect on premixed, laminar flame speed, in agreement with theory and other observations [27].

For each trial, the flame reached the wall before the vessel vented, however, the time between those two events decreased substantially with increasing R32 concentration. This general linear trend can be observed for all three starting pressures, although the venting times were consistently longest for the 81.1 kPa starting pressure (triangles in Figure 3.2) and shortest for the 101.3 kPa starting pressure (circles). A richer mixture of R32 in air will result in more heat released and higher temperatures in the vessel, in addition to a greater number of moles of products produced; in a control volume, both of these factors contribute to a higher pressure in the vessel. This explains the downward trend in venting time as a function of concentration. For the lowest tested concentrations, no venting time is marked because the vessel did not vent prior to flame extinction. These trials only vented upon the forced injection of air to evacuate the contents of the flask.

One test at 101.3 kPa was not included in this figure because the concentration, 16%, was well above the LFL for R32. In this case, the flame hit the wall at approximately 0.24 s and the vessel vented at 0.25 s. These two events are almost simultaneous, within the accuracy of $\pm$ 1 frame of the high speed video.

In all the experiments performed, the flame reaches the wall of the flask before venting. This behavior is attributed to the weight of the stopper. These events occur closer together with increasing concentration and starting pressure, suggesting the rate of rise influences the venting pressure. At a pressure above atmospheric, or a concentration closer to stoichiometric (17.4%), it seemed likely that the flask would vent well before the flame reached the wall. More testing could confirm this. If the vessel has already vented before the flame hits the wall of the vessel, the flame

propagation could be altered and the angle of the flame could no longer be accurately representative for the concentration. Caution should be taken to only analyze tests in which the flame reaches the wall of the sphere prior to venting, although this will require a change to ASTM E681. Decreased starting pressure would reduce the likelihood of premature venting for a wider range of concentrations, but the reduced starting pressure may have a noticeable effect on flame propagation, as will be discussed in a later section.

3.2 Electrode Quenching Effects on Pressure

One significant difference between the glass and polycarbonate test setups was the positioning of the electrodes, as shown in Figure 3.4. For the glass vessel, the electrodes came in vertically through the neck of the flask. For the polycarbonate vessel, the electrodes were drilled horizontally into the side of the sphere.

Figure 3.4: Vertical electrodes in glass (left) and horizontal electrodes in polycarbonate (right)

While the quenching impact of the electrodes has been speculated by other researchers, the effects have never been quantified [18, 28, 29]. R32 has a quenching distance of approximately 7 mm, which is higher than typical hydrocarbons such as propane with a quenching distance of approximately 2 mm [30]. For 3 mm diameter electrode rods spaced 32 mm apart, 7 mm quenching distance is significant.

Initial comparisons of data from the glass and polycarbonate vessels at 101.3 kPa starting pressure suggested a significant effect of electrode placement. This was illustrated through the two different sets of pressure curves in Figure 3.5. The evolution of pressure was plotted as a function of time for a sample of flame propagation trials.
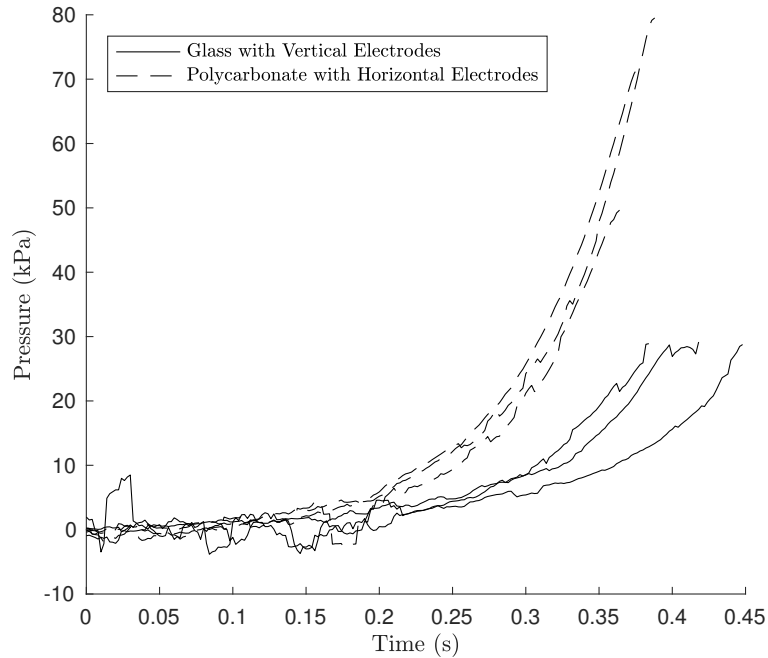

Figure 3.5: Discrepancy between 14.8% R32 flame for glass and polycarbonate

Both sets of tests were conducted at atmospheric pressure with the same concentration of 14.8% R32. The results were reproducible; the three vertical electrode

curves show the same shape as each other, and the three horizontal electrode trials were almost identical. The difference in maximum pressure was explained by the venting mechanism, not the electrodes, but the differences prior to venting were influenced by the location of the electrodes. An experiment was performed to quantify the quenching effects of the metal rods on the flame by inserting a pair of metal rods, without a spark gap at the end, into the polycarbonate vessel, as shown in Figure 3.6.
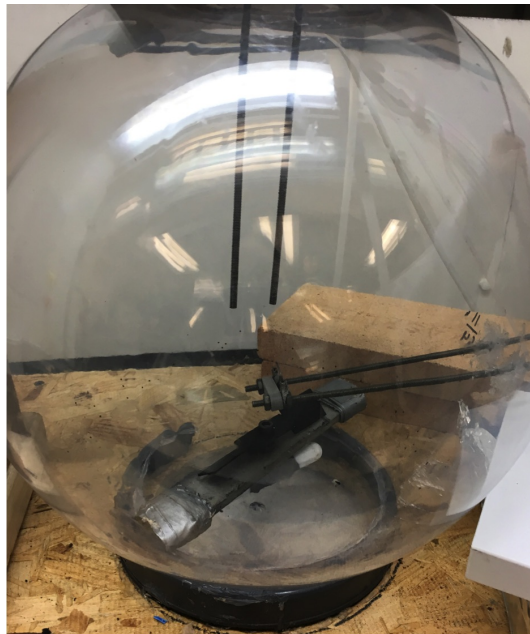
Figure 3.6: Vertical rods incorporated into polycarbonate apparatus with horizontal electrodes

Distinction from Standard   A distinction between the experimental apparatus and the ASTM E681 apparatus must be made here. The standard calls for the electrodes to be surrounded by a glass sheath to reduce the likelihood of arcing. Both of the test configurations showed no evidence of arcing between the rods, so this glass casing was not included on either system. Because neither system had

glass sheathing, they can be directly compared to each other. Furthermore, the glass would substantially increase the diameter of the electrode rods, which would only *increase* the magnitude of quenching effects if included.

Comparisons between glass, polycarbonate, and the modified polycarbonate apparatus are featured in Figure 3.7 for tests of 14.0%, 14.4%, and 14.8% R32 at 101.3 kPa starting pressure.

The top plot in Figure 3.7 compared three pressure curves, representative of the vertical electrodes in glass, the horizontal electrodes in polycarbonate, and the hybrid configuration in polycarbonate. Only one trial was shown for each case, but the results were all repeated with one representative case featured. The addition of two dummy electrodes into the flame path reduced the difference between the two curves. The pressure in the vessel rose faster for the case without electrodes in the flame path, suggesting a clear impact of quenching. Quenching occurs when a surface absorbs heat and free radicals from the flame, which both reduce the ability for a flame to propagate. R32 and other mildly flammable refrigerants have quenching distances on the order of several millimeters. The electrodes were responsible for weakening the flame. The impact of the electrodes must be considered for future revisions to the ASTM E681 standard test equipment.

The same pattern was observed for 14.4% R32, the middle plot in Figure 3.7. The original discrepancy between the polycarbonate and glass arrangements was less than the 14.8% case, but the additional vertical electrodes again accounted for this discrepancy.
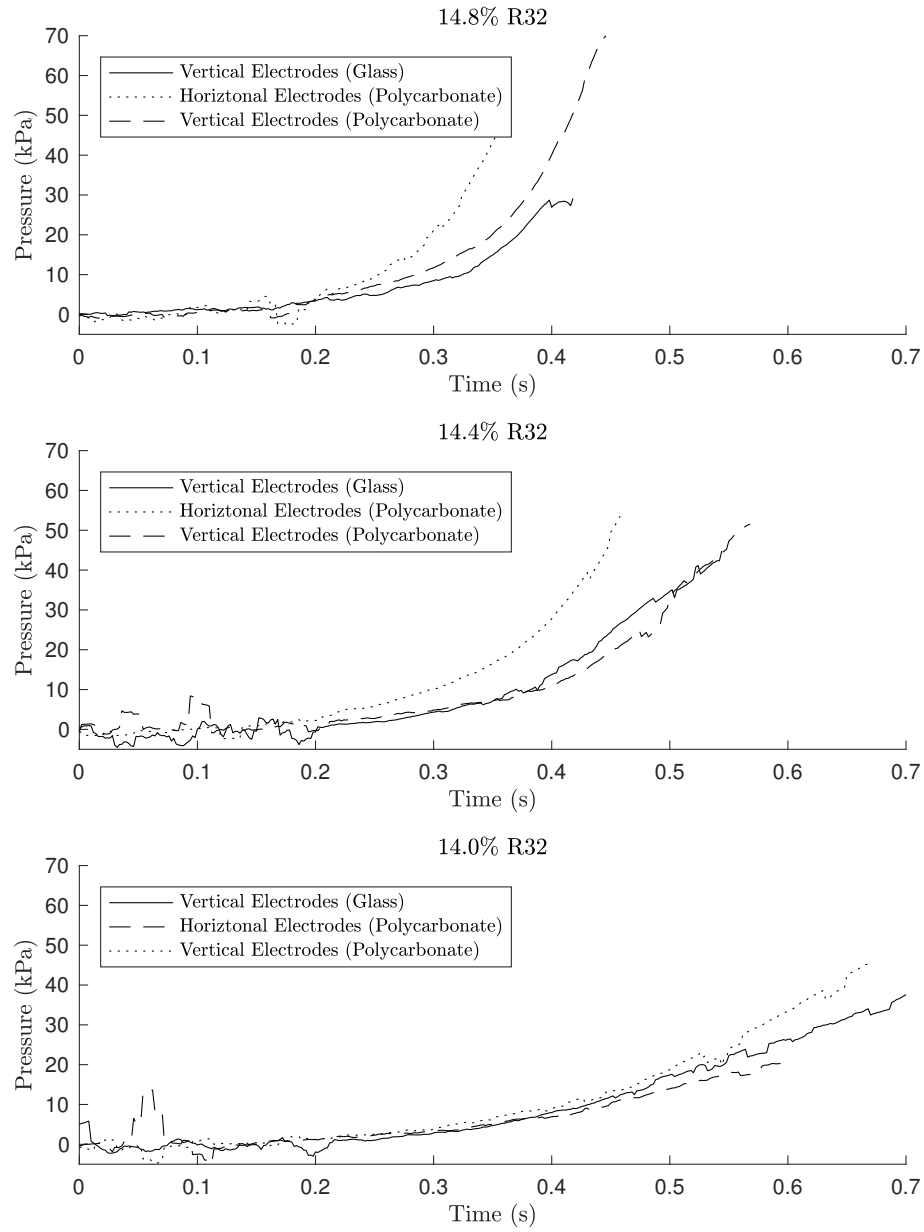
Figure 3.7: Electrode quenching effects for various concentrations at 101.3 kPa
initial pressure

For 14.0% R32, there was little difference between the glass and polycarbonate systems. The arrangement with additional electrode rods does not cause further deviation. Comparisons between the 14.8%, 14.4%, and 14.0% cases suggest that the electrodes had an increasing impact on flame propagation with increasing concentration though the physical justification is not known. Reported values for the LFL of R32 were generally between 14% and 15%; significant impact of the electrodes was observed on this range, so it cannot be neglected for identifying the LFL for future refrigerant composition developments.

Comparisons between the visual propagation differences for the different configurations are described at length in the thesis by Jonathan Reymann [26].

3.3 Pressure Measurements and Flammability Determination

The main focus of this research was pressure and its ability to characterize flammability and propagation behavior. Measurements were taken for a range of concentrations surrounding the LFL of R32 to identify key metrics that could define flammability. In addition to the effects of concentration, the effects of initial pressure were also examined. All experiments discussed in the following section were taken from the polycarbonate apparatus; this eliminates variations that would result from electrode placement or venting mechanism.

3.3.1 Effects of Initial Pressure

The ASTM E681 test is generally performed with the contents initially at atmospheric pressure (101.3 kPa), but there was little literature to address variations in initial pressure below atmospheric pressure. These fluctuations could represent altitude variations as well as test condition variations. Local weather pressure in College Park, MD fluctuated between 99 and 104 kPa over the course of this study.

A series of measurements were taken for starting pressures of 81.1, 91.2, and 101.3 kPa. Several metrics were evaluated to understand the impact of concentration and initial pressure on refrigerant flammability. The venting of the system limits the full potential of pressure analysis because the flame might have continued to burn the contents of the flask and raise the pressure in the mixture had venting not occurred. Despite this limitation, meaningful observations could still be made.

3.3.1.1 Fractional Pressure Rise

One common metric for flammability limits was a fractional pressure rise. Fractional pressure rise was calculated as

$$Rise = \frac{P_{final}}{P_{initial}},\tag{3.2}$$

where P_{final} was the pressure at the moment of venting and $P_{initial}$ was the initial pressure at the moment of ignition. Both pressures were measured in absolute kPa. This can accommodate different starting pressures. Figure 3.8 shows fractional

pressure rise as a function of concentration for all three starting pressures.

For each starting pressure represented in Figure 3.8, the overall pressure rise started low and increased until a plateau level above 40% pressure rise. One clear limitation of this analysis was venting. Once the apparatus vents, the pressure can no longer continue to rise. For this reason, limited distinction can be made using this metric between concentrations above a certain concentration, as summarized in Table 3.1. This concentration is labelled as a 'critical' concentration instead of an LFL because this is not an official flammability definition.

Table 3.1: Critical Concentrations for Percent Pressure Rise

Starting Pressure	Critical Concentration
101.3 kPa	14.0%
91.2 kPa	13.9 - 14.0%
81.1 kPa	14.2 - 14.5%

From previous research, it is understood that flammability limits widen with increasing starting pressure. With decreased starting pressure, flammability limits are expected to narrow. The effects of starting pressure were evident here. The difference between 91.2 kPa and 101.3 kPa was insignificant, but the behavior at 81.1 kPa was noticably different. While a lower starting pressure was beneficial because more of the flame's propagation was captured before venting, the impacts of starting pressure must be addressed. In terms of percent pressure rise, 91.2 and 101.3 kPa were both reasonable substitutes for each other, but 81.1 kPa would not be as representative of the same flame development.
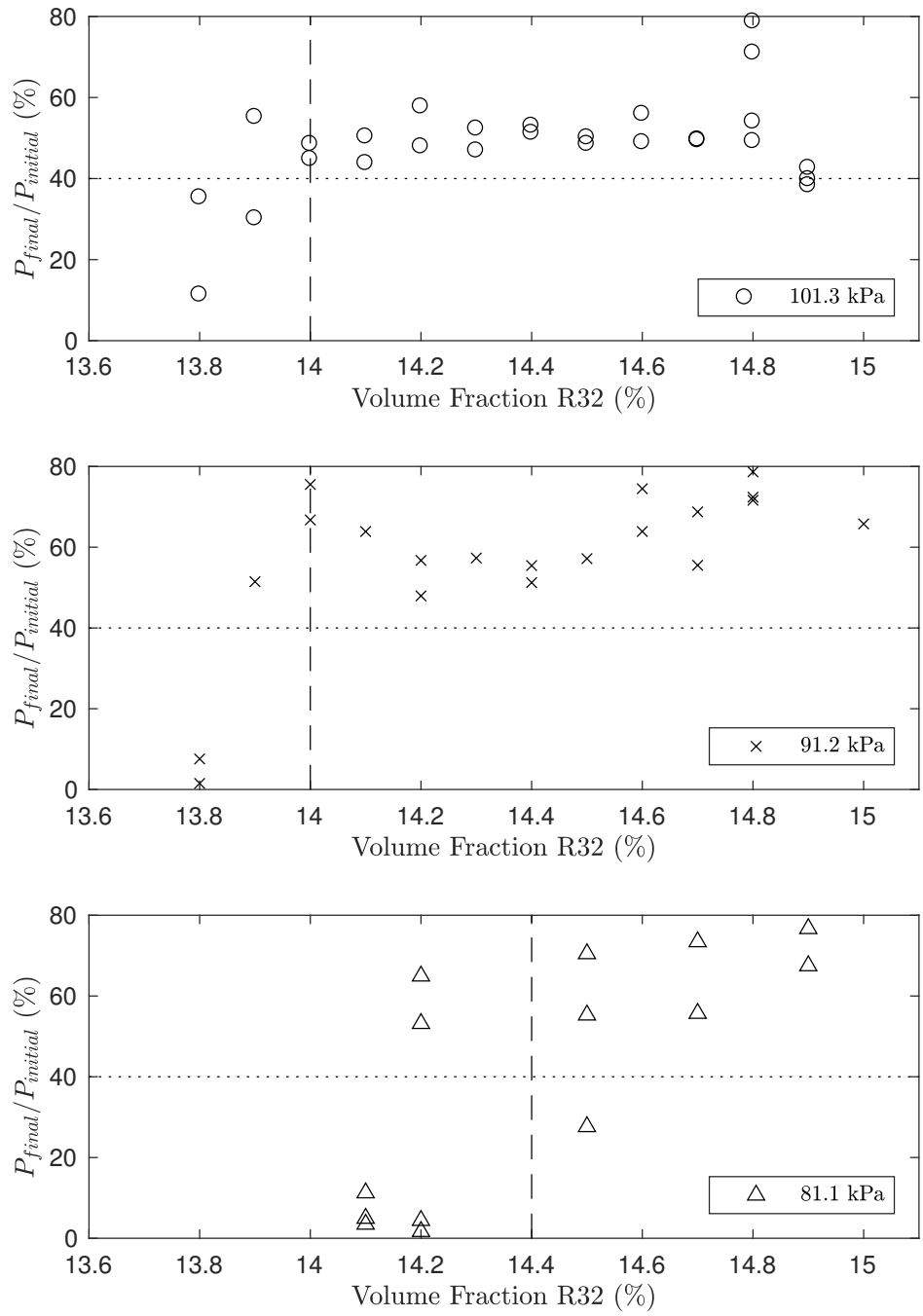
Figure 3.8: Pressure rise as a percentage of initial pressure

3.3.1.2   Rate of Pressure Rise

Another metric for flammability was the rate of pressure rise. As a flame propagates through a mixture, the pressure in the sealed container also increases. A rapidly propagating flame with a wide flame angle will burn the contents of the vessel faster, thus raising the pressure in the flask quickly. Three different rates of pressure rise will be examined for each of the three starting pressures.

Each derivative of pressure added noise to the measurements. The rate of pressure rise was the first derivative of pressure with respect to time. The two measurements were compared in Figure 3.9 for a trial of 14.8% R32 at 101.3 kPa initial pressure.
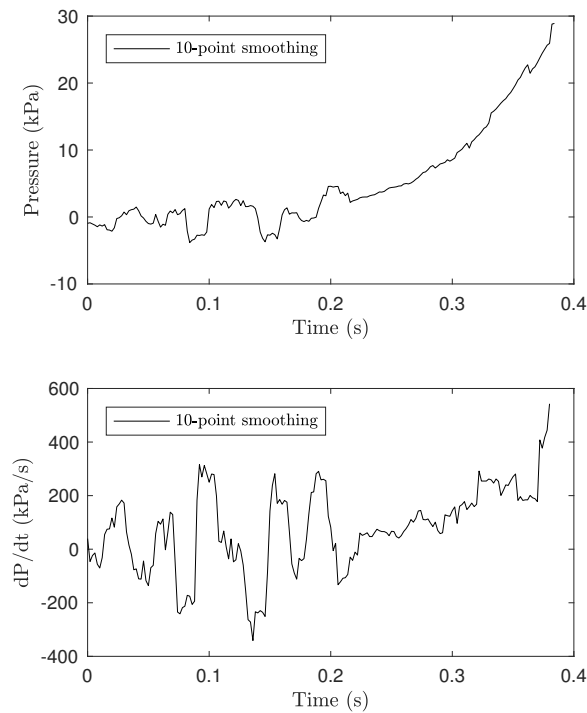

Figure 3.9: Pressure measurement (top) and rate of pressure rise (bottom) for 14.8% R32 with 101.3 kPa initial pressure

Both plots were displayed with a 10-point running average filter. The noise level increased with the derivative. To minimize these effects, the three rates of pressure rise that were considered were calculated as averages between the end points of the time interval.

The first rate of pressure rise was the average rate of pressure rise, taken from the moment of ignition to the moment of maximum pressure. The measurements for the average rate of pressure rise show an upward trend in pressure rise as a function of concentration for all three starting pressures, as seen in Figure 3.10. Initial values are low, corresponding to the same concentrations where the pressure rise was less than 40% of the initial concentration. After this threshold, the trend is generally linear for the average rate of pressure rise as a function of concentration. There is little distinction between the rates of pressure rise for 91.2 and 101.3 kPa, though the rates of rise for 81.1 kPa starting pressure are consistently lower than those for higher starting pressures.
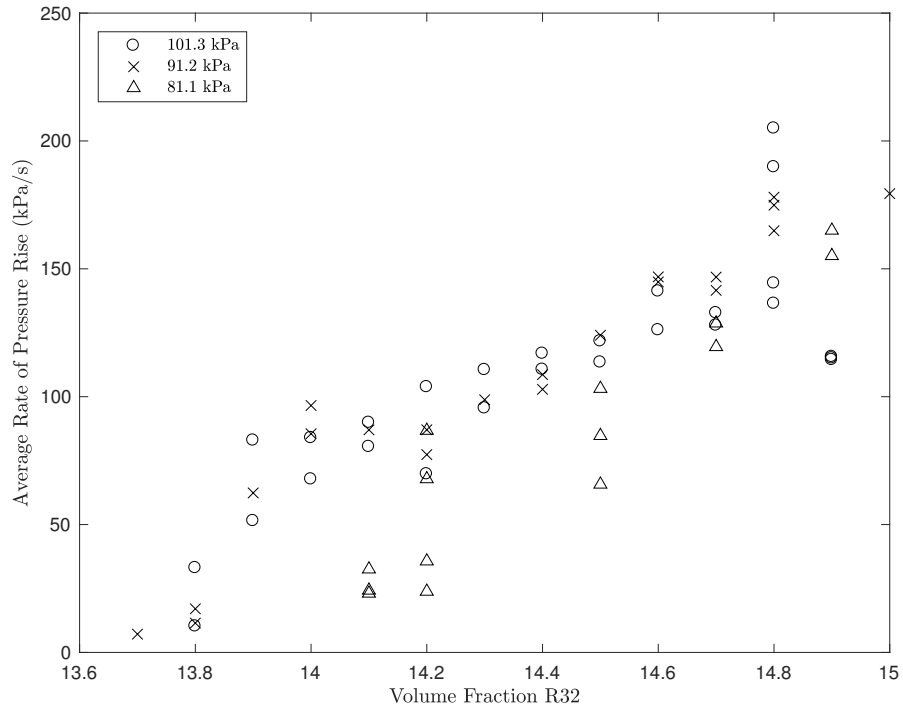
Figure 3.10: The average rate of pressure rise from ignition to venting

The second rate of pressure rise was the final rate, defined for the last 0.05 s prior to venting. This was an approximation for maximum rate of pressure rise, since the instantaneous rate of rise is noisy. The maximum rate of pressure rise increased with increasing concentration, as highlighted in Figure 3.11. For this metric, a clear distinction was seen for each starting pressure. The final rates of pressure rise were highest for 101.3 kPa starting pressure and lowest for 81.1 kPa starting pressure. For 81.1 and 91.2 kPa, the trends were generally linear with no limiting value. For 101.3 kPa starting pressure, the trend was linear up until a point where it plateaued, around 450 kPa/s. At this point, the rate of pressure rise caused the vessel to vent, generally around a pressure of 50 kPa. The two maximum values at 14.8% occurred due to an unusually high venting pressure.
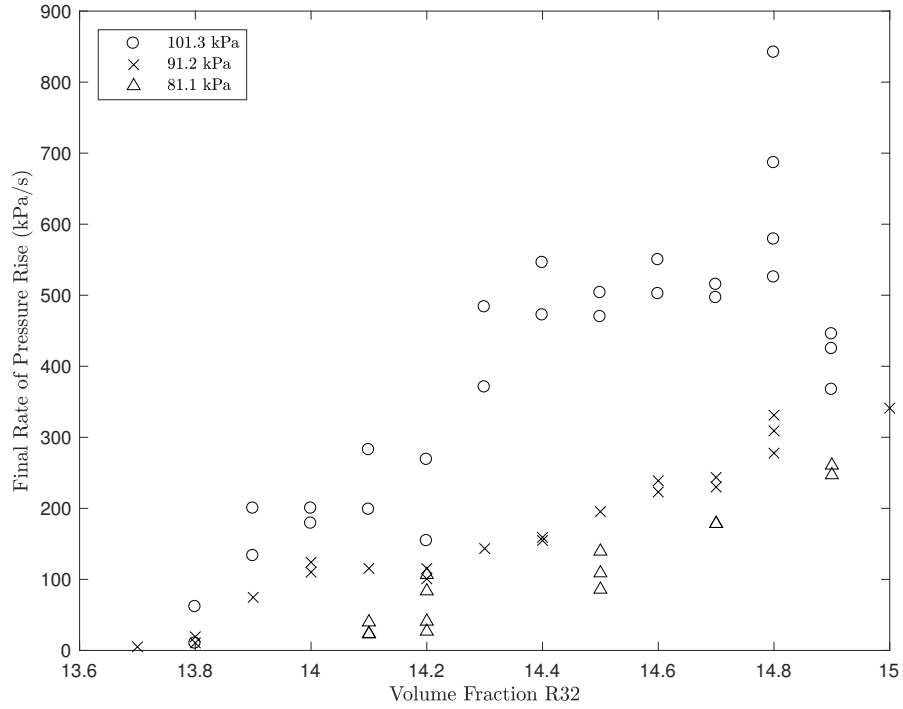
Figure 3.11: The average rate of pressure rise for the last 0.05 s prior to venting

The third examined rate of pressure rise was the instantaneous rate of pressure rise once the pressure in the vessel had risen by 20 kPa above its starting pressure. Almost every mixture passes 20 kPa before venting, and the curves were generally distinguishable from each other at this point. This rate of pressure rise was calculated by finding the time when the pressure reached 17.5 kPa and the time where the pressure reached 22.5 kPa and evaluating the rate of rise between those two points as an approximate value for the rate of rise centered around 20 kPa,

$$\left.\frac{dP}{dt}\right|_{P=20kPa} = \frac{5\ kPa}{t_{22.5kPa} - t_{17.5kPa}}.$$ (3.3)

44

Like the previous two rates of pressure rise, an increasing trend was observed with increasing concentration for all three starting pressures. The trend was less linear than the other two rates of pressure rise. Because of the high rates of pressure rise and the limited sample rate (500 Hz), several points laid directly on top of each other. This rate of pressure rise showed a much more scatter at each concentration than the previous two metrics, however, this rate of pressure rise was not dependent on venting pressure, which allows more independence from the venting mechanism. Little distinction could be made for the measurements above 14.4% R32, with a rate of pressure rise greater than or equal to 200 kPa/s. Additionally, this metric showed negligible distinction between 81.1, 91.2 and 101.3 kPa starting pressures.
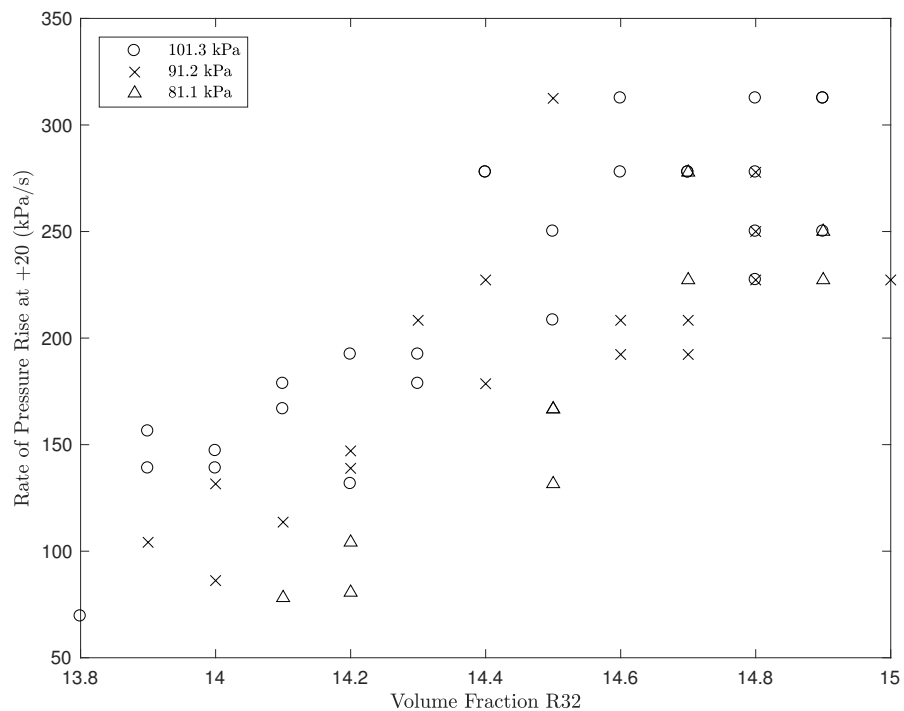

Figure 3.12: The instantaneous rate of pressure rise when the pressure has risen +20 kPa

45

3.3.2 Recommended Initial Pressure

An initial pressure of 91.2 kPa will be beneficial for the ASHRAE 34 and ASTM E681 standard test. This starting pressure is representative of atmospheric pressure, as explained in this chapter, but reduces the likelihood of premature venting. The visual criteria is evaluated when the flame reaches the walls of the vessel. By synchronizing the high speed footage with the pressure data, the pressure in the flask at this moment was measured. For concentrations near the currently established LFL (14.4%), the pressure at this critical moment is near 110 kPa, as illustrated in Figure 3.13.
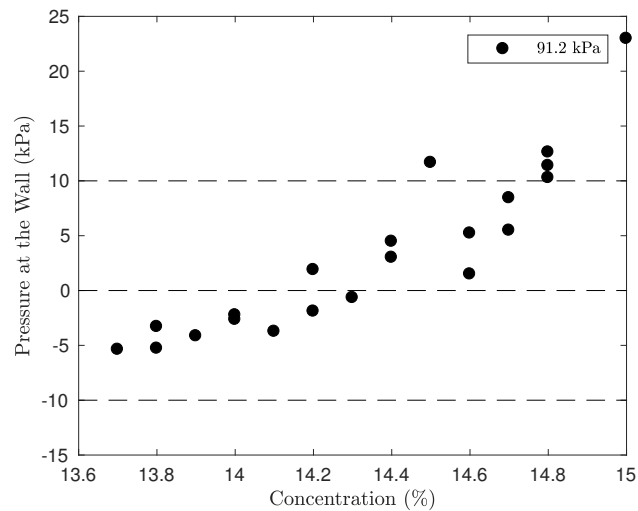

Figure 3.13: Measurements of gauge pressure in the vessel when the flame reaches the wall for a 91.2 kPa initial pressure

This would center the test around atmospheric pressure (101.3 kPa) which would be another benefit to the standard because it would represent an average of atmospheric conditions.

3.3.3 LFL Criteria for R32

More work will be required to define a flammability limit criteria that is applicable to all 2L refrigerants, but one can be reasonably derived for R32. A hypothetical criterion can be proposed around each analyzed metric at 91.2 kPa starting pressure, and the validity of each as an objective measure of flammability was addressed.

Figure 3.8 showed the sharpest distinction with concentration. Fractional pressure rise above atmospheric starting pressure was evaluated. A distinction existed at 14.0% R32. Below this concentration, almost no propagation was observed and the vessel rarely vented in these cases. Above this concentration, a sharp rise in pressure was observed and the system vented after a minimum of 40% pressure rise. This criterion was dependent on venting pressure and was not able to distinguish between pressures above 14.0%. These were both limitations of the metric, though the sharp jump at 14.0% indicated a physical difference in propagation, so this criteria would be a reasonable dividing line between flammable and non-flammable mixtures.

The average rate of pressure rise, taken from ignition to venting, was linear with concentration. In this way, any criterion established on this metric must be arbitrary. A pressure rise of 125 kPa/s would create a division between flammable and non-flammable mixtures around 14.4% which is the current industry standard LFL for R32. This metric was dependent on venting pressure, so its application was limited by the venting behavior of the apparatus at the specific testing laboratory.

The final rate of pressure rise, taken for the last 0.05 s prior to venting, showed

a linear trend and a rate of rise of 200 kPa/s could be a reasonable cutoff to meet current industry standards. Again, this rate of rise was dependent on venting pressure and each derivative of pressure adds noise to the signal.

The local rate of pressure rise when the mixture reaches 20 kPa above the starting pressure showed a series of plateauing values around 14.5% R32 in air. This rate of pressure rise at +20 kPa was not dependent on the venting pressure, which allowed for repeatable results despite variations in venting mechanism on each individual test apparatus. Variations were possible due to sampling rate or the exact method of calculating the rate of pressure rise, but these parameters could be standardized. This method was limited, though, by its inability to distinguish between concentrations above 14.5%, corresponding to a rate of pressure rise greater than or equal to 200 kPa/s.

Ultimately, the most applicable metric for defining flammability was fractional pressure rise of 40%. The criterion showed a sudden increase at a given concentration, which was indicative of a change in flammability. Fractional pressure rise was simple to evaluate and the strategy was most common throughout the literature. Noise develops through evaluating derivatives, limiting the application of rate-based criteria into a standard test method. More testing must be done across different laboratories and with a series of different refrigerants to make sure that this metric shows visible distinctions for more refrigerants than R32. Additionally, UFL testing must be performed to make sure the chosen criterion holds up for concentrations above stoichiometric.

3.3.3.1 Comparison to Visual Criteria

For the same series of tests, J. Reymann [26] analyzed high speed video footage to measure flame angles, per the method described in ASTM E681. Flame angle was plotted against R32 concentration. A linear fit was established across the data set and the point where the trend line crossed 90° was considered to be the LFL. This matched with the 2/3 rule for flame propagation criteria in ASTM E681 [3]. For 101.3 kPa, the LFL was found to be 14.6%. For 91.2 kPa, the LFL was found to be 14.8% [26]. For 81.1 kPa, a final LFL was not determined, but it would be significantly above 14.9% R32. Through visual and pressure criteria, 81.1 kPa was not representative of atmospheric conditions, based on both visual and pressure criteria.

The minimal variation here between 91.2 and 101.3 kPa starting pressure for flame angle suggests that either could be used for testing conditions. Because 101.3 kPa starting pressure captures a shorter duration of flame propagation prior to venting, 91.2 kPa would be a beneficial substitute for 101.3 kPa test conditions.

Both flame angle measurements were higher than the proposed LFL of 14.0% using the 40% fractional pressure rise determination. The lower LFL is more conservative, which can have a safety benefit when designing systems to protect from flammability hazards.

3.3.3.2 Comparison to Literature Data

Previously established flammability limits for R32 from the literature were compared to the values derived from potential pressure-based LFL criteria. Through Kondo's work using visual criteria, LFL of 13.5% and 13.8% were found [16,17]. These values were low compared to other literature values.

Using a twin counterflame setup, Grosshandler and co-workers [15, 23, 24] reported an LFL of 14.0% for R32. This was consistent with the findings of this study for a 40% pressure rise.

Zhang and Wilson [1,19] both reported an LFL of 14.4%, which is considered the current industry standard for R32. In the current study, this corresponded to the criteria derived from the rate of pressure rise at 20 kPa greater than or equal to 200 kPa/s.

Finally, previous tests in this laboratory at the University of Maryland yielded an LFL of 14.7% and 14.8% of R32 using the glass ASTM E681 apparatus [8]. With the modified polycarbonate apparatus and an initial pressure of 91.2 kPa, Reymann reported an LFL of 14.8% [26]. These values for LFL exceed the values derived from the proposed pressure-based LFL criteria.

This current study proposes criteria that result in more conservative estimates for LFL than the ASTM E681 standard, but the estimates are still within the accepted range of existing literature. More experiments should be done to compare refrigerants beyond R32, but this foundation suggests that a suitable pressure criteria can be created to align with the 90° visual criteria.

3.4   Pressure Summary

Venting behavior was well-characterized through audio and pressure measurements. The quenching effects of the electrode rods were significant on the development of the flame and increased with concentration. In the current ASTM E681 standard, these effects of premature venting and quenching are not addressed.

The percent pressure rise as well as three different rates of pressure rise were compared across different concentrations and initial pressures. For the average pressure rise and the final rate of pressure rise, the results are highly dependent on the venting pressure. Because the venting pressure was not consistent for the apparatus, the application of these metrics were limited. Although the trends were less linear than other metrics, the rate of pressure rise as the mixture passed +20 kPa was a viable metric for characterizing the flame propagation because it was not effected in any way by the venting pressure of the vessel.

For fractional pressure rise, average rate of pressure rise, and pressure rise at +20 kPa, the results of 91.2 and 101.3 kPa starting pressure were indistinguishable. For every examined metric, 81.1 kPa produced noticeably different results. The primary goal of this research was to improve and refine the LFL for atmospheric conditions, and 81.1 kPa is not representative of atmospheric conditions, based on pressure criteria.

The most applicable metric for defining flammability was fractional pressure rise of 40%. The criterion showed a sudden increase at a given concentration, which was indicative of a change in flammability. Fractional pressure rise was simple to

evaluate and the strategy was most common throughout the literature. The criterion depends on venting pressure, but this can be controlled with a weighted stopper. An initial test pressure of 91.2 kPa would improve the repeatability of the standard by minimizing the risk of premature venting and keeping the test centered around 101.3 kPa. More testing must be done across different laboratories and with a series of different refrigerants to make sure that this metric shows visible distinctions for more refrigerants than R32. Additionally, UFL testing must be performed to make sure the chosen criterion holds up for concentrations above stoichiometric.

Chapter 4: Conclusion and Recommendations for Future Work

The ASHRAE 34 and ASTM E681 standards have limitations that need to be addressed. Venting precautions, starting pressure effects, quenching losses, and pressure-based flammability criteria were analyzed.

Venting was analyzed for the use of a weighted stopper. The point of maximum pressure and an audio signature were both valid methods to identify the moment of venting. It was found that the flame reached a critical distance, the walls of the flask, prior to venting for concentrations near the LFL. This was observed for 81.1, 91.2 and 101.3 kPa, but the clearance between the time of reaching the walls and venting was higher with lower initial pressures. The length of time between the flame reaching the walls and the vessel venting decreased with both increasing concentration and increasing starting pressure. If a visual criteria remains in the standard, caution must be taken to ensure that the analysis always takes place prior to venting.

Quenching losses due to the electrode placement were significant and could be seen in pressure development. Electrode placement must be modified for future revisions to the ASHRAE 34 standard due to the high quenching distances for A2L refrigerants.

Starting pressures below atmospheric were analyzed to understand the impact on pressure development from flame propagation. Lower starting pressures allowed more of the flame propagation to be captured prior to venting, but an impact was found as a function of starting pressure. For most analysis metrics, 91.2 and 101.3 kPa starting pressures were good approximations of each other. Critical points for pressure rise criteria and visual flame angles were only separated by 0.1-0.2% by concentration. This was within the repeatability expectations for the standard, so either starting pressure can be used. A recommendation will be made to the standard to incorporate an initial pressure of 91.2 kPa. This will allow for consistency within and between labs and more confidence in venting time, without a loss in applicability to atmospheric pressure conditions.

Finally, the visual flammability criteria for the ASTM E681 standard is subjective and dependent on camera settings, frame rate, and lighting. A pressure-based flammability criteria was suggested: a total pressure rise of 40% (30% would create a similar dividing line). The total pressure rise was dependent on the final venting pressure of the apparatus, so this may be a limitation, however, the sharp increase at 14.0% concentration suggests a physical change indicative of a fundamental flammability limit; an LFL of 14.0% would be reported as the LFL using this method. This pressure-based criteria was validated by some literature values for R32 flammability limits, though the value was more conservative than the current industry standard.

This work suggests that an appropriate pressure-based criteria can be derived that will be reasonably consistent with the current ASTM E681 results. Pressure-based criteria will be more objective and independent of flask material, as long as

electrode placement is consistent and venting is controlled. Before fully incorporating pressure-based criteria into the standard, further testing should be conducted to validate the methods with other refrigerants and refrigerant blends. Humidity and temperature effects should be considered. Humidity was a negligible factor for R32, but has a significant impact on other refrigerants. Testing should also be conducted across a few different testing laboratories to quantify reproducibility of results.

Appendix A: ASTM E681 Glass Apparatus with Burst Disk

A.1   Apparatus Details

An ASTM E681 12 L glass apparatus was used for some baseline testing. The apparatus can be seen in Figure A.1.
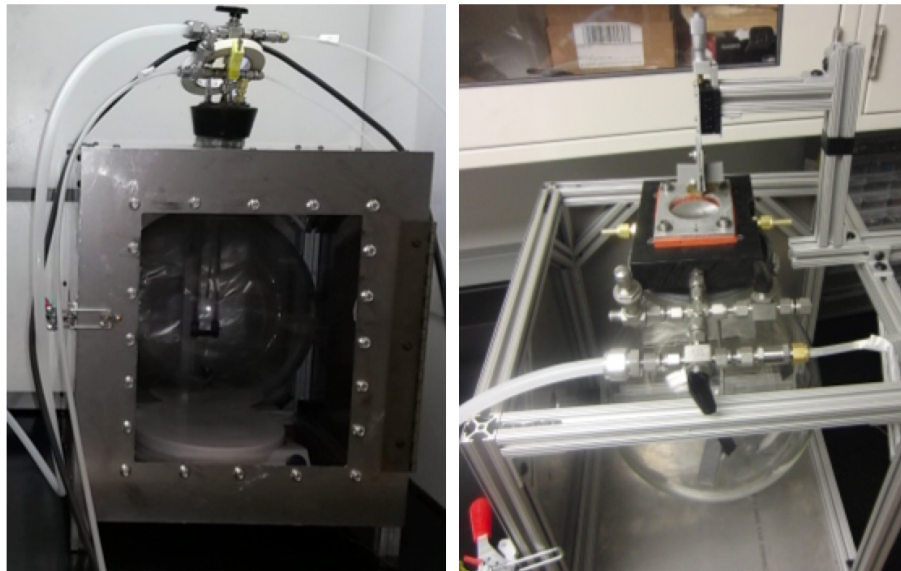

Figure A.1: Glass apparatus (left) with modified burst disk for venting (right)

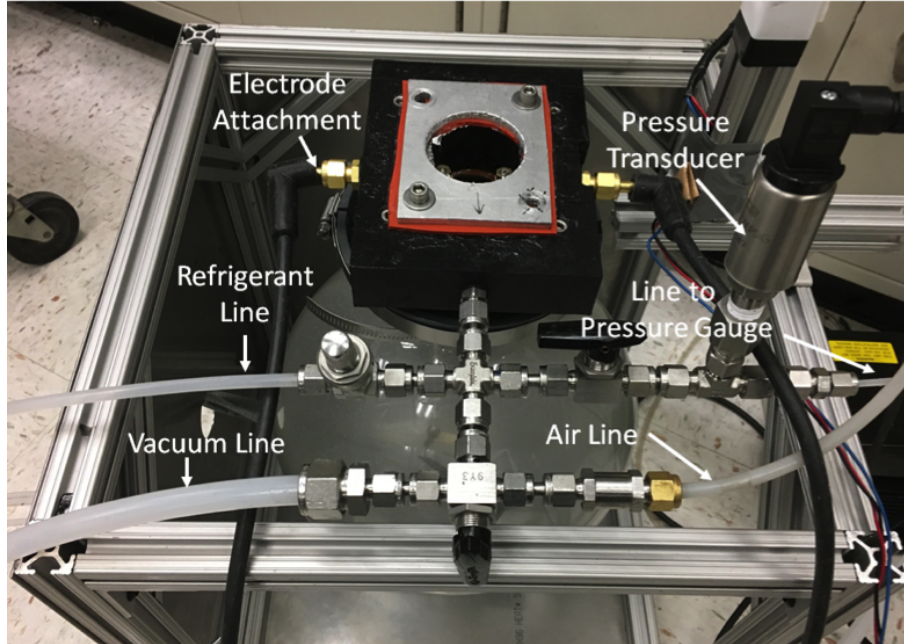Instrumentation and key features are labelled in Figure A.2.

Figure A.2: Labeled plumbing tee, attached to the burst disk

A.2   Burst Disk Venting Analysis

The venting mechanics were different for the apparatus with the burst disk and the apparatus with the weighted stopper. Two microphones were used, side by side, to record the audio from the experiments performed with the burst disk apparatus. A typical experiment for 14.8% R32 generates the plots shown in Figure A.3.
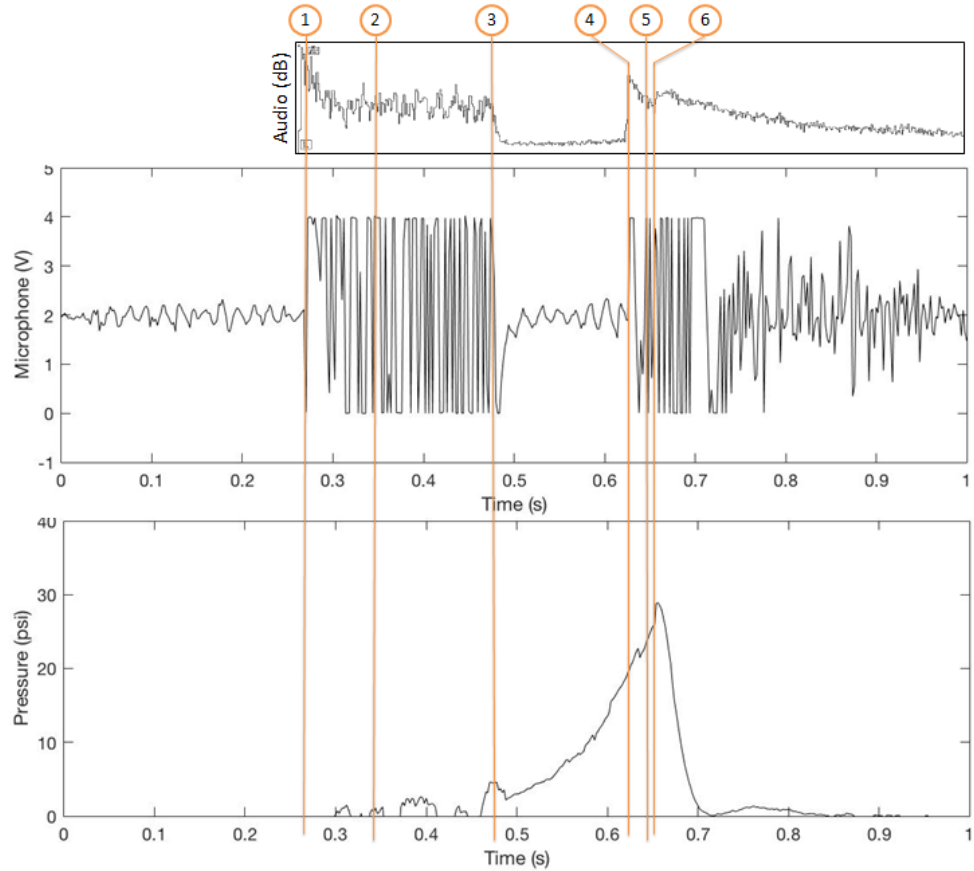
Figure A.3: Burst disk venting with two microphones and a pressure transducer for 14.8% R32; (1) spark begins, (2) flame kernel is visible, (3) spark ends, (4) initial puncture, (5) flame reaches the wall, and (6) full venting occurs

The top plot shows the lapel microphone; the middle plot shows the voltage amplifier microphone; the bottom plot shows the pressure transducer. Six key events were marked on the plot; these six events correspond to the six flame stills in Figure A.4.
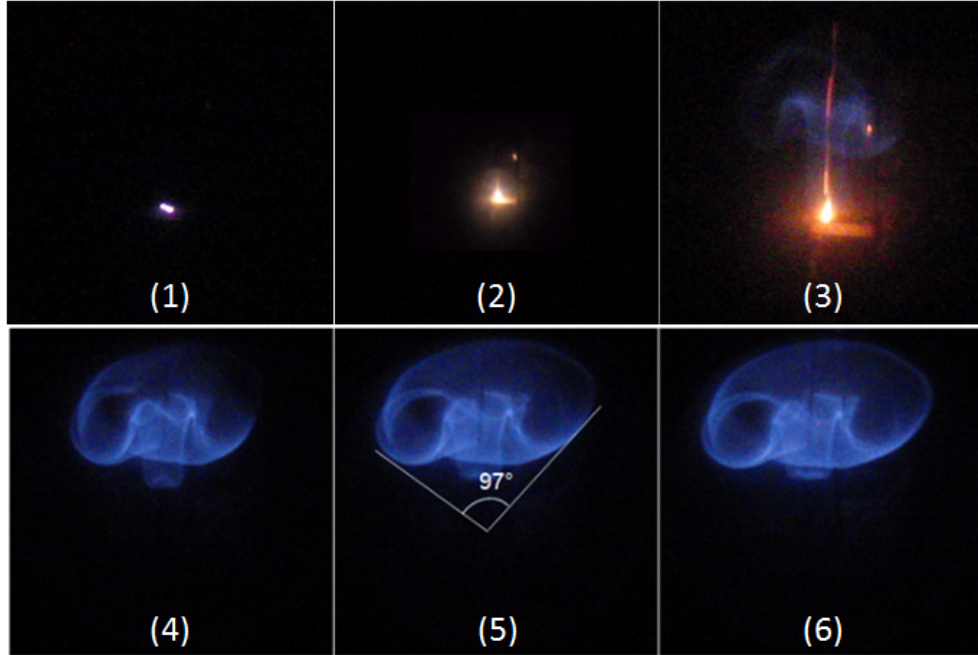
Figure A.4: Flame propagation photos; key events (1) spark begins, (2) flame kernel is visible, (3) spark ends, (4) initial puncture, (5) flame reaches the wall, and (6) full venting occurs

Ambient sound levels were recorded before the first event. The first event was the initiation of the spark, as noted in both audio plots. The second was the first visual sign of flame propagation identified in the high speed video. The third event was the end of the 0.2 s period of spark generation. It should be noted that the spark signature looks different in this plot compared to Figure 3.1. Both audio signatures in Figure A.3 are affected by RF noise, so it shows an overly amplified sound during spark generation. For timing, however, it still represented the duration of the spark accurately. The next key event was the first venting sound (puncture). Next, the flame reached the walls of the flask. Finally, the full pop of the burst disk was heard.

Two distinct sounds were heard during the venting of the burst disk. The first was named the 'puncture' because the knife edge makes a small hole in the

foil at this point. The puncture has a negligible impact on flame propagation. The second sound was named the 'pop' because it seemed louder to the operators and it corresponded to a large hole being opened in the burst disk. This had a clear visual impact on flame propagation. The short time between the moments of puncture, flame reaching the walls, and burst indicate a potential limitation of the system.

The lapel microphone was abandoned by the time the polycarbonate vessel was in use. It was redundant and more confidence existed in the Adafruit microphone. Furthermore, the weighted stopper venting did not exhibit two phases, puncture and burst, but only one sound of full venting, so the lapel microphone detail was not necessary.

Bibliography

[1] David P. Wilson and Robert G. Richard. Determination of refrigerant lower flammability limits in compliance with proposed addendum p to Standard 34. *ASHRAE Transactions 2002*, 108(2):739–756, 2002.

[2] *ANSI/ASHRAE Standard 34-2013: Designation and Safety Classification of Refrigerants.* ASHRAE, Atlanta, GA, 2013.

[3] ASTM International. Standard test method for concentration limits of flammability of chemicals (vapors and gases). Technical Report E681-09, ASTM International, West Conshohocken, PA, January 2010.

[4] Volkmar Schröder and Maria Molnarne. Flammability of gas mixtures, Part 1: Fire potential. *Journal of Hazardous Materials*, A121:37–44, 2005.

[5] ASTM International. Standard practice for determining limits of flammability of chemicals at elevated temperature and pressure. Technical Report E918-83, ASTM International, West Conshohocken, PA, 2011.

[6] United Nations. Globally harmonized system of classification and labelling of chemicals (GHS). Technical Report ST/SG/AC.10/30/Rev.4, United Nations, New York and Geneva, 2011.

[7] *NFPA 69: Standard on Explosion Prevention Systems.* National Fire Protection Association, Quincy, MA, 2014 edition, 2014.

[8] Conor G. McCoy. *Improved Venting for Flammability Limit Testing Using ASTM E681 Apparatus.* Master of science, University of Maryland, College Park, Maryland, 2016.

[9] Peter Quillen Lomax. *Development of the ASTM E681 Standard.* Master of science, University of Maryland, College Park, Maryland, 2016.

[10] F. Van den Schoor, R.T.E. Hermanns, J.A. van Oijen, F. Verplaetsen, and L.P.H. de Goey. Comparison and evaluation of methods for the determination of flammability limits, applied to methane/hydrogen/air mixtures. *Journal of Hazardous Materials*, 150:573–581, May 2007.

[11] Isaac A. Zlochower and Gregory M. Green. The limiting oxygen concentration and flammability limits of gases and gas mixtures. *Journal of Loss Prevention in the Process Industries*, 22:499–505, March 2009.

[12] Daniel A. Crowl and Young-do Jo. A method for determining the flammable limits of gases in a spherical vessel. *Process Safety Progress*, 28(3):227–236, April 2009.

[13] Xueling Liu and Qi Zhang. Influence of initial pressure and temperature on flammability limits of hydrogen-air. *International Journal of Hydrogen Energy*, 39:6774–6782, February 2014.

[14] Zhenming Li, Maoqiong Gong, Eryan Sun, Jianfeng Wu, and Yuan Zhou. Effect of low temperature on the flammability limits of methane/nitrogen mixtures. *Energy*, 36:5521–5524, August 2011.

[15] W.L. Grosshandler, M.K. Donnelly, and C. Womeldorf. Flammability measurements of difluoromethane. San Diego, CA, March 15-19 2000. ASME.

[16] Shigeo Kondo, Kenji Takizawa, and Kazuaki Tokuhashi. Effects of temperature and humidity on the flammability limits of several 2L refrigerants. *Journal of Fluorine Chemistry*, 144:130–136, 2012.

[17] Shigeo Kondo, Akifumi Takahashi, Kenji Takizawa, and Kazuaki Tokuhashi. On the pressure dependence of flammablity limits of CH2=CFC3, CH2F2 and methane. *Fire Safety Journal*, 46:289–293, April 2011.

[18] Everett W. Heinonen and Robert E. Tapscott. Methods development for measuring and classifying flammability/combustibility of refrigerants. Interim Report DOE/CE/23810-42G, The Center for Global Environmental Technologies New Mexico Engineering Research Institute, Albuquerque, New Mexico, June 1994.

[19] Wang Zhang, Zhao Yang, Jin Li, Chang-xing Ren, and Dong Lv. Study of the explosion characteristics and combustion products of air conditioner using flammable refrigerants. *Journal of Fire Sciences*, 33(5):405–424, 2015.

[20] I. Kul, D.L. Gnann, A.L. Beyerlein, and D.D. DesMarteau. Lower flammability limit of difluoromethane and percolation theory. *International Journal of Thermophysics*, 23(4):1085–1095, July 2004.

[21] Robert G. Richard. Refrigerant flammability testing in large volume vessels. Technical Report DOE/CE/23810-87, Buffalo Research Laboratories, Buffalo, New York, March 1998.

[22] Ya A. Lisochkin and V.I. Poznyak. Explosion hazard of mixtures of freons R31 and R32 with air at different pressures. *Combustion, Explosion and Shock Waves*, 37(4):448–450, 2001.

[23] Carole Womeldorf, Michelle King, and William Grosshandler. Lean flammability limit as a fundamental refrigerant property. Interim Technical Report - Phase I DOE/CE/23810-58, National Institute of Standards and Technology, Gaithersburg, MD, March 1995.

[24] W.L. Grosshandler, M.K. Donnelly, and C. Womeldorf. Flammability measurements of difluoromethane in air at $100^{o}C$. San Diego, CA, March 15-19 2000. ASME.

[25] Everett W. Heinonen and Robert E. Tapscott. Methods development for measuring and classifying flammability/combustibility of refrigerants. Final Report DOE/CE/23810-42G, The Center for Global Environmental Technologies New Mexico Engineering Research Institute, Albuquerque, New Mexico, December 1994.

[26] Jonathan Reymann. *Improvements to refrigerant flammability limit testing with ASTM E681 through the use of a polycarbonate testing apparatus*. Master of science, University of Maryland, College Park, Maryland, 2017.

[27] Irvin Glassman, Richard A. Yetter, and Nick G. Glumac. *Combustion*. Elsevier, fifth edition, 2015.

[28] Guenther Vol Elbe. The Problem of Ignition. *Symposium (International) on Combustion*, 4(1):13–20, 1953.

[29] Bin Bai, Zheng Chen, Huangwei Zhang, and Shiyi Chen. Flame propegation in a tube with wall quenching of radicals. *Combustion and Flame*, 160:2810–2819, July 2013.

[30] Kenji Takizawa, Akifumi Takahashi, Kazuaki Tokuhashi, Shigeo Kondo, and Akira Sekiya. Burning velocity measurement of fluorinated compounds by the spherical-vessel method. *Combustion and Flame*, 141:298–307, March 2005.